

Frascati Physics Series Vol. VVVVVV (xxxx), pp. 000-000  
 XX CONFERENCE – Location, Date-start - Date-end, Year

## IDENTIFICATION OF SHOWERS WITH THE CORE OUTSIDE THE ARGO-YBJ DETECTOR

Giuseppe Di Sciascio, Elvira Rossi on behalf of the ARGO-YBJ Collaboration  
*Dip. di Fisica Università di Napoli and INFN, sez. di Napoli, Italy*

### ABSTRACT

In this paper we present a procedure able to identify and reject showers with the core outside the ARGO-YBJ carpet boundaries. The efficiency of this method is investigated for different primary energies and fiducial areas. A comparison of the results for gamma and proton induced showers is also presented.

### 1 Introduction

The ARGO-YBJ detector, currently under construction at the Yangbajing Laboratory (P.R. China, 4300 m a.s.l.), is a full coverage array of dimensions  $\sim 74 \times 78 \text{ m}^2$  realized with a single layer of RPCs. The area surrounding this central detector (*carpet*), up to  $\sim 100 \times 110 \text{ m}^2$ , is partially ( $\sim 50\%$ ) instrumented with other RPCs. The basic element is the logical *pad* ( $56 \times 62 \text{ cm}^2$ ) which defines the time and space granularity of the detector. The layout of the

detector is shown in Fig. 1. The detector is subdivided in  $6 \times 2$  RPC units (Clusters, the rectangles of Fig. 1).

Showers of sufficiently large size will trigger the detector even if their core is located outside its boundaries. The corresponding core positions are generally reconstructed not only near the carpet edges but also well inside them. As a consequence, sophisticated algorithms to reduce the contamination of external events are needed. The goal is to identify and reject a large fraction of external events before exploiting any reconstruction algorithm only by using some suitable parameters.

The rejection of external events is important because a large difference between the true and the reconstructed shower core position may lead to a systematic miscalculation of some shower characteristics, such as the shower size. Moreover, an accurate determination of the shower core position for selected internal events is important to reconstruct the primary direction using conical fits to the shower front, improving the detector angular resolution or to perform an efficient gamma/hadron discrimination.

In this paper we present a reconstruction procedure able to identify and reject a large fraction of showers with core outside the ARGO-YBJ detector. The efficiency of this procedure is investigated both for gamma and proton induced showers.

## 2 Identification of external events

To perform these calculations we have simulated, via the Corsika code <sup>1)</sup>,  $\gamma$ -induced showers with a Crab-like spectrum ( $\sim E^{-2.5}$ ) and proton events with  $\sim E^{-2.75}$ , both ranging from 100 GeV to 50 TeV. The  $\gamma$ -rays have been simulated for different zenith angles ( $< 40^\circ$ ), following the daily path of the source in the sky. The detector response has been simulated via a GEANT3-based code. The core positions have been randomly sampled in an area, energy-dependent, large up to  $800 \times 800 \text{ m}^2$  centered on the detector.

In Fig. 2 we show the fraction of showers with the core truly internal (external) to a fiducial area approximately equal to the carpet dimensions ( $A_{fid} = 80 \times 80 \text{ m}^2$ ) as a function of the number of pads fired on the ARGO-YBJ carpet. The upper plot refers to  $\gamma$ -induced showers, the lower to proton-induced events. As expected, for low pad multiplicities the events are mainly external: about 40% of the  $\gamma$ -induced showers with a multiplicity of 100 - 150

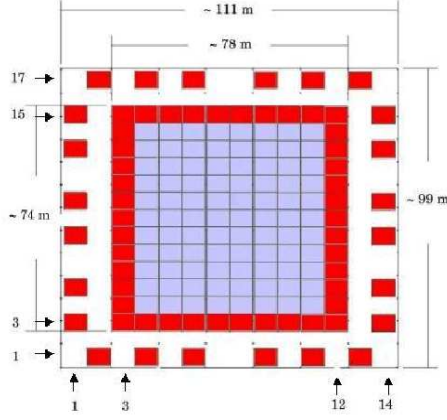


Figure 1: *The ARGO-YBJ detector.*

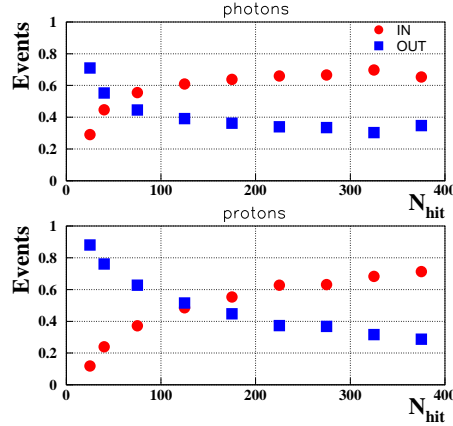


Figure 2: *Fraction of events with the core IN (OUT)  $A_{fid} = 80 \times 80 \text{ m}^2$ .*

fired pads are external to  $A_{fid}$ . But also for higher multiplicities the percentage of external events is consistent (about 30%).

Various parameters based on particle density or time information are under investigation to identify showers with core position outside a given fiducial area<sup>2)</sup>. In this paper we discuss the performance of the following ones:

- Position of the cluster with the highest particle density.
- Position of the cluster row/column with the highest particle density.
- Mean distance  $R_p$  of all fired pads to the reconstructed shower core position.

As an example, in Fig. 3 we show the distributions of the positions of the cluster with the highest particle density for  $\gamma$ -induced showers which fire more than 100 pads on the central carpet. In the plots we compare the events with the core truly external to a  $80 \times 80 \text{ m}^2$  fiducial area (solid histograms) and the truly internal ones (dashed histograms). To investigate the discrimination power of this particular parameter we have simulated a detector completely instrumented up to  $\sim 100 \times 110 \text{ m}^2$ , i.e., containing  $14 \times 17$  clusters. Therefore, the cluster coordinates run from 1 to 14 (X view) and from 1 to 17 (Y view) starting from the lower left corner of the carpet (see Fig. 1). The clear

difference between the IN and OUT showers suggests to tag as external the events with the highest particle density in the outer clusters and to reject them before exploiting any reconstruction algorithm.

The mean lateral spread of the shower can be expressed as:

$$R_p = \frac{\sum_{i=1}^N |r_C - r_i| n_i}{\sum_{i=1}^N n_i} \quad (1)$$

where  $N$  is the number of fired pads,  $r_C$  is the reconstructed core position,  $r_i$  is the position of the  $i$ -th fired pad,  $n_i$  is the number of detected electrons in the  $i$ -th pad. The  $R_p$  distribution for showers reconstructed inside a  $80 \times 80$  m<sup>2</sup> fiducial area is shown in Fig. 4 (solid histogram). The dashed line refers to truly IN events while the dotted histogram refers to OUT showers erroneously reconstructed as internal. The shower cores have been calculated by means of the simple center of gravity method. As can be seen, the parameter  $R_p$  identifies quite well the events with core outside the carpet. Large distances between the true and the reconstructed shower axis lead to larger  $R_p$  values. This fact offers the possibility to define a cut in  $R_p$  to identify these events. A conservative choice is to reject showers with  $R_p > 25$  m.

From these studies it follows that the identification of a large fraction of external events can be achieved by defining a suitable fiducial area and a combination of cuts in the parameters discussed above.

### 3 Maximum Likelihood Method (LLF)

Different algorithms have been investigated to reconstruct the shower core position in the ARGO-YBJ experiment <sup>3)</sup>. The most performant one is the Maximum Likelihood Method.

If  $\langle m_i \rangle$  is the average particle number expected on the  $i$ -th pad, then the probability of finding  $N_i$  particles is

$$P_i = \frac{\langle m_i \rangle^{N_i}}{N_i!} \cdot e^{-\langle m_i \rangle} \quad (2)$$

Therefore  $P_i(0) = e^{-\langle m_i \rangle}$  is the probability of finding 0 particles, and  $P_i(>0) = 1 - e^{-\langle m_i \rangle}$  is the probability of finding 1 or more particles. The Likelihood Function (LF) is given by:  $LF = \prod_i P_i$ . The natural Logarithm of LF (LLF) becomes a sum:

$$LLF = \ln(\prod_i P_i) = \sum_i \ln P_i(0) + \sum_j \ln P_j(>0) \quad (3)$$

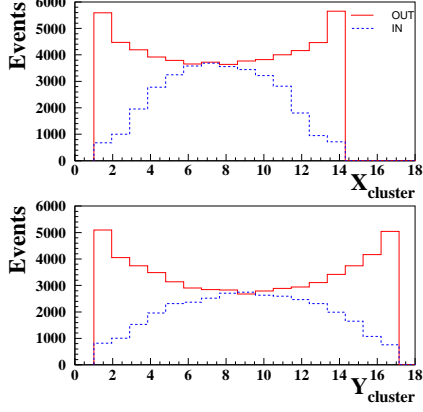


Figure 3: *Coordinate distributions of the cluster with the highest particle density for  $\gamma$ -induced events with pad multiplicity  $N_{hit} > 100$ .*

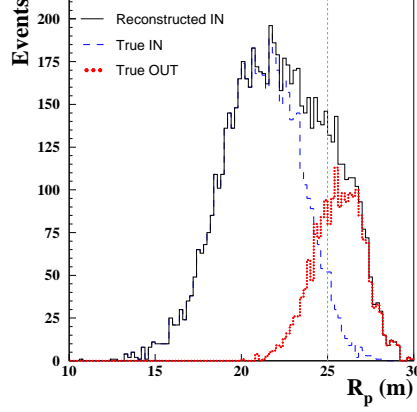


Figure 4: *Distributions of the parameter  $R_p$  for  $\gamma$ -induced events with  $N_{hit} > 100$ .*

where the index  $i$  runs on the not fired pads, while the index  $j$  refers to the fired pads. Exploiting the relation  $\langle m_i \rangle = S_{pad} \cdot \rho_i$ , we obtain

$$-LLF \equiv S_{pad} \cdot \sum_i \rho_i - \sum_j \ln(\rho_j) - N_{pad}(> 0) \cdot \ln(S_{pad}) \quad (4)$$

where  $\rho_i = f(R_i/R'_M) \cdot \frac{N_e}{R'^2_M}$  is the particle density expected on the  $i$ -th pad at a distance  $R_i$  from the core. The lateral structure function  $f(R_i/R'_M)$  has been calculated for the ARGO-YBJ detector:

$$f\left(\frac{R_i}{R'_M}\right) = C \cdot R_i^{A-2} \cdot \left(1 + \frac{R_i}{R'_M}\right)^{-B} \quad (5)$$

with the normalization factor defined by

$$C = \frac{\Gamma(B)}{2\pi(R'_M)^{A-2}\Gamma(A)\Gamma(B-A)} \quad (6)$$

where  $R'_M = R_M/3.944$ ,  $R_M$  being the Moliere radius (133 m at YBJ altitude), and  $A = 1.826$ ,  $B = 2.924$ ,  $C = 0.613$ .  $S_{pad}$  is the pad area and  $N_{pad}(> 0)$  is the total number of pads fired by the shower. The minimum value of -LLF is then chosen as the best fit for the freely varying parameters  $\{x_c, y_c, N_e\}$ , being

$\{x_c, y_c\}$  the core coordinates and  $N_e$  the shower size. In the following we will refer to this approach as to the "LLF1 method".

We point out that expression (4) for -LLF refers to the case of a Poisson distribution in which the pads are not fired with probability  $P_i(0)$  or fired with probability  $P_i(> 0) = 1 - P_i(0)$ . In our study almost always the fired pads have particle multiplicity 1, and therefore such a simple discrimination can be made. However, if we consider a larger area as the whole RPC, the multiplicity can also be  $> 1$ , and the proper Poisson distribution on the fired RPCs appears more adequate. In this case the sum on fired elements is:

$$-\Sigma_j \ln P_j(> 0) = -\Sigma_j N_j \ln(\rho_j) - \ln(S_{RPC}) \Sigma_j N_j + \Sigma_j \ln(N_j!) + S_{RPC} \Sigma_j \rho_j \quad (7)$$

where  $\rho_j$  is the particle density expected on the  $j$ -th RPC at a distance  $R_j$  from the core,  $N_j$  is the recorded particle number and  $S_{RPC}$  is the RPC area. The shower size can be calculated via the equation

$$N_e = \frac{\Sigma_j N_j}{S_{RPC} \Sigma_j \rho_j} \quad (8)$$

We call this calculation the "LLF2 method". As a consequence, we expect that the differences between LLF1 and LLF2 increase, for a fixed area, with the particle density. In Fig. 5 we compare the shower core position resolution  $\sigma_{core} = \sqrt{\sigma_x^2 + \sigma_y^2}$  calculated by applying the LLF1 and LLF2 methods on the RPCs for  $\gamma$ -induced showers with the core randomly sampled inside a  $80 \times 80 m^2$  area. As expected, the resolution worsens with the multiplicity if the LLF1 approach is applied when the number of particles hitting the RPC is  $> 1$ . We note that for very low multiplicities ( $N_{hit} < 80$ ) method LLF1 is more performant than LLF2. Indeed, the algorithm based on the RPC occupancy (LLF1) provides a better representation of the hit distribution in very poor showers. For very high multiplicities ( $N_{hit} > 10^3$ ) the shower core position is determined by LLF2 with an uncertainty  $< 1 m$ .

In Fig. 6  $\sigma_{core}$  obtained with the LLF2 method is shown as a function of multiplicity for  $\gamma$  and proton induced showers with core randomly sampled in an area, energy-dependent, large up to  $800 \times 800 m^2$ . The fiducial area is  $80 \times 80 m^2$ . The increase of the sampling area worsens the performance of the method because of the contamination by external events (see Fig. 2). This effect can be limited exploiting the cuts described in section 2. As an example, in Fig. 7 we compare the shower core position resolutions for  $\gamma$  and

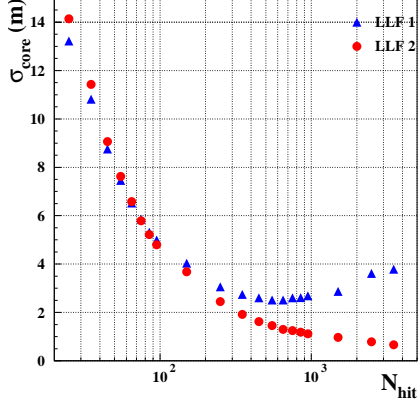


Figure 5: Comparison between the shower core position resolutions obtained with LLF1 and LLF2 methods.

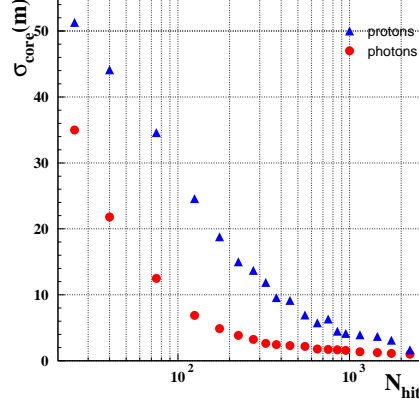


Figure 6: Shower core position resolutions obtained with LLF2 for  $\gamma$  (circles) and proton (triangles) showers.

proton showers after the following selection procedure: (1) Rejection of the events whose highest density clusters are on the guard ring ( $X = \{1, 14\}$ ;  $Y = \{1, 17\}$ ) or on the boundaries of the central carpet ( $X = \{3, 12\}$ ;  $Y = \{3, 15\}$ ); (2) Rejection of the events whose highest total density rows or columns are respectively in positions  $\{1, 3, 15, 17\}$  or  $\{1, 3, 12, 14\}$ ; (3) Reconstruction of core coordinates  $\{X_c, Y_c\}$  using LLF2; (4) Further rejection of events with  $R_p > 25$  m.

For events with a multiplicity of  $100 - 150$  hits  $\sigma_{core}$  improves from  $6.9$  to  $4.4$  m for  $\gamma$ -induced showers and from  $24.6$  to  $21.3$  m for proton events. For any given multiplicity the shower core position resolution is better for  $\gamma$  than for proton induced showers, due to the larger lateral particles spread in the latter.

## 4 Results

The procedure (1) - (4) is one of the possible procedures to reject external events in the ARGO-YBJ detector. In Fig. 8 the fraction of rejected events (internal and external to  $A_{fid} = 80 \times 80$  m<sup>2</sup>, respectively) is reported for  $\gamma$  and proton-induced showers. As can be seen, this algorithm is able to identify and

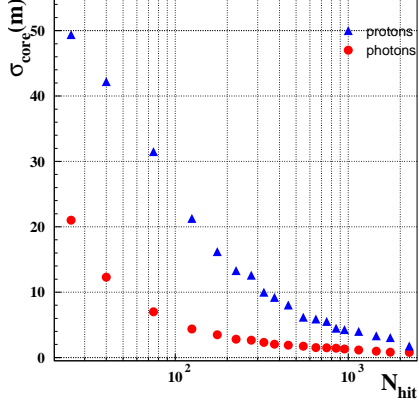


Figure 7: Comparison between the shower core position resolutions for  $\gamma$  (circles) and proton (triangles) events after the selection procedure (1) - (4).

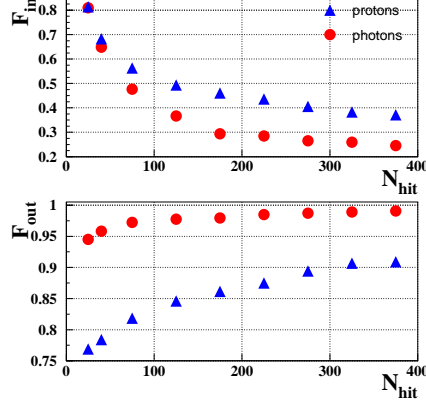


Figure 8: Fraction of truly internal ( $F_{in}$ ) and external ( $F_{out}$ ) events rejected by the selection procedure (1) - (4).

reject a large fraction of external events: for photons this percentage is always larger than 95%. For low multiplicities ( $N_{hit} < 150$ ) a significative fraction of internal events is erroneously rejected, especially in proton-induced showers.

The fraction of internal and external events rejected with the above procedure is shown for different fiducial areas, separately for  $\gamma$ -induced showers (Fig. 9) and for proton-induced events (Fig. 10). The fraction of discarded showers increases with  $A_{fid}$  mainly at high multiplicities. For  $\gamma$ -showers more than 94% of external events are rejected for the investigated fiducial areas. The fraction of internal events erroneously rejected is less than 30% for high multiplicities ( $N_{hit} > 150$ ). The performance of the procedure is lower for proton showers.

Due to the larger lateral particles spread in proton showers the  $\gamma$ /hadron relative trigger efficiency is smaller for external events than for internal ones. Thus, a suitable choice of the fiducial area  $A_{fid}$  may improve the overall detector sensitivity to point  $\gamma$ -ray sources even if the total effective area is decreased.

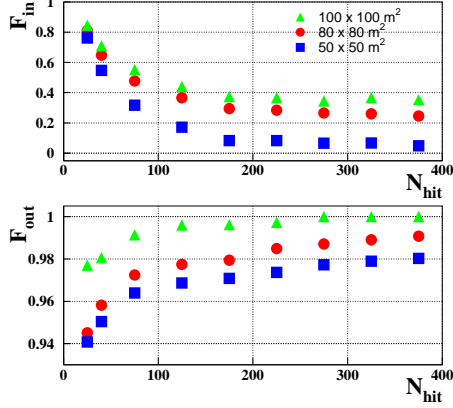


Figure 9: *Fraction of truly internal ( $F_{in}$ ) and external ( $F_{out}$ )  $\gamma$  showers rejected by the selection procedure (1) - (4) for different fiducial areas.*

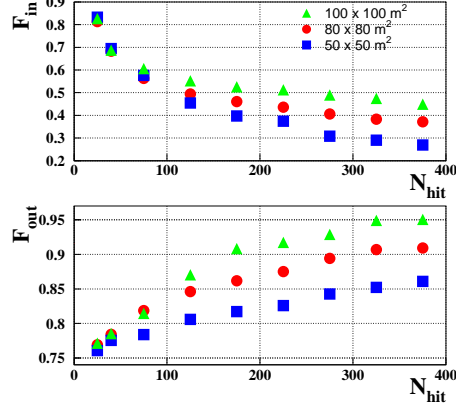


Figure 10: *Same as Fig. 9 but for proton showers.*

## 5 Conclusions

The fraction of external events which triggers the ARGO-YBJ detector is relevant, mainly for low multiplicities (see Fig. 2). In this paper we discussed a possible procedure to tag and reject a relevant fraction of external showers before the calculation of the shower core position via the LLF2 method, thus saving CPU time. We applied this algorithm to a sample of  $\gamma$ -induced showers with a Crab-like energy spectrum. For comparison, we studied the performance of the procedure for proton-induced showers with an energy spectrum  $\sim E^{-2.75}$ .

With a suitable choice of the fiducial area and applying simple cuts we can reject more than 94% of the external  $\gamma$  showers and more than 80% of the external proton events, saving more than 50% of the internal events (for  $N_{hit} > 70$ ). As a consequence, we expect an improvement in the reconstruction of some shower characteristics, such as the primary direction <sup>4</sup>).

## References

1. D. Heck et al., Report **FZKA 6019** Forschungszentrum Karlsruhe.

2. E. Rossi, University Degree Thesis, Naples (2002), unpublished.
3. Martello D., Bleve C. and Di Sciascio G. 2001, 27th ICRC, Hamburg, 7, 2927.
4. G. Di Sciascio and E. Rossi, *Study of the angular resolution of the ARGO-YBJ detector*, these proceedings.